High-frequency Floquet-theory content of wave-packet dynamics

J. C. Wells,[1] I. Simbotin,[1] and M. Gavrila[1,2]
[1]*Institute for Theoretical Atomic and Molecular Physics, Harvard-Smithsonian Center for Astrophysics, Cambridge, Massachusetts 02138*
[2]*FOM Institute for Atomic and Molecular Physics, Kruislaan 407, 1098 SJ, Amsterdam, The Netherlands*
(Received 18 February 1997)

We study the connection of the high-frequency Floquet theory (HFFT) and the wave-packet dynamics (WPD) descriptions of laser-atom interactions. The analysis is motivated by the need to ascertain the realm of validity of the current form of the HFFT and extend its scope. We test the general ideas on a one-dimensional atomic model with soft Coulomb potential, frequently considered before. The comparison is carried out in two stages of approximation. In the first stage, we compare WPD predictions for ionization with those from the usual (single-state) form of the HFFT. To make the comparison meaningful, we use as initial conditions for the WPD bound high-frequency ''dressed states,'' corresponding to the peak intensity of the field. The dressed states play a special role in the HFFT and have direct physical interpretation at high frequencies. We show that, under certain conditions, the decay rates extracted from WPD agree rather well with those from the HFFT. Thus ''adiabatic stabilization,'' derived originally from the HFFT, results also from WPD. This form of the phenomenon contrasts ''dynamic stabilization,'' the only form shown so far to follow from WPD. In the next stage of the comparison, we extend the HFFT in two directions: we include results from the second iteration within the theory, and we introduce a multistate HFFT analysis. As a test for the agreement of the HFFT and WPD we compare the results regarding the populations in dressed states. In a variety of circumstances we find striking agreement, indicating the potential of the multistate Floquet analysis. In addition, we study the characteristics of the population trading among the dressed states during the ionization process. Although the individual populations in bound states may fluctuate substantially, their sum decreases rather smoothly in time, as predicted analytically by the HFFT. [S1050-2947(97)02311-1]

PACS number(s): 42.50.Hz, 32.80.Wr, 33.80.Wz

I. INTRODUCTION

The theory of laser-atom interactions at high intensities has been developed using basically two approaches [1]. One is Floquet theory, which assumes a regime of steady ionization and calculates the constant decay rates from a spatial boundary-value problem [2]. The other is wave-packet dynamics (WPD), i.e., the integration of the time-dependent Schrödinger equation with given initial conditions [3]. The information they give is of complementary nature in the quantum-mechanical sense: Floquet theory emphasizes the energy domain and WPD the time domain. Both have known merits and limitations; e.g., see [1]. However, only a dual approach based on both can give definitive answers to the delicate physical problems that abound in strong-field laser-atom interactions. For example, Floquet theory has made exotic predictions as to the behavior of atoms in intense fields (adiabatic stabilization, light-induced states, etc.). Some of them may be hard to accept unless substantiated by standard WPD, particularly because Floquet theory with resonance (Gamow-Siegert) boundary conditions operates with wave functions having unbounded behavior at infinity. The dual approach is needed also for understanding the conditions under which an experimental confirmation of Floquet theory predictions can be expected.

We shall be interested here in the connection between Floquet theory and WPD at high frequencies and constant field amplitude. A version of Floquet theory specifically adapted for this case is the ''high-frequency Floquet theory'' (HFFT), developed by Gavrila and Kaminski [4,5]. It proceeds iteratively, yielding successive approximations of higher order in ω^{-1} [6]. A central role in the possibility of comparing WPD and HFFT is played by the initial condition of WPD, which has to be adapted to the assumptions under which the HFFT operates. To make the comparison meaningful, we shall analyze the initial condition in terms of superpositions of ''dressed states,'' which are limiting forms of Floquet states at high frequency. These play a structural role in the HFFT and have direct physical interpretation.

We shall proceed with the comparison of WPD and HFFT in two stages, corresponding to two successive levels of accuracy in the development of the HFFT. In the *first stage*, we shall be using the HFFT in its current form (i.e., single state and including only the first iteration in ω^{-1}). We shall compare the ionization rates of the two theories, corresponding to the same initial condition and, in particular, we shall dwell on the phenomenon of atomic stabilization. The HFFT has predicted the existence of ''*adiabatic stabilization*'' [7], characterized by the fact that, for individual atomic states adjusting adiabatically to the variation of the laser intensity, beyond a critical intensity the ionization rates start to decrease and the states become more stable. This has been meanwhile confirmed by all Floquet methods in existence [8]. Moreover, the onset of adiabatic stabilization was confirmed experimentally for Rydberg atoms [9]. On the other hand, WPD has produced its own version of stabilization, termed ''*dynamic*'' [10,11]. In this version, when an intense laser pulse is suddenly applied to an atom in the ground state, its total ionization probability exhibits stabilization as the peak intensity is increased. It has not been shown, however, that adiabatic stabilization also followed from WPD. We shall show here that this is indeed the case.

 © 1997 The American Physical Society

For the *second stage* of our comparison, we extend the HFFT theory in two respects: We include results from the second iteration in ω^{-1} within the HFFT and introduce the *multistate HFFT*. Whereas the first extension is conceptually simple, the second requires delicate mathematical arguments. The extension relies on the mathematical *completeness* of Floquet (in our case high-frequency Floquet) states, i.e., the possibility of expanding wave packets in terms of such states. For periodic time-dependent Hamiltonians, this is the counterpart of the completeness property for time-independent Hamiltonians, which plays a fundamental role in the interpretation of quantum mechanics. Whereas the completeness property of Floquet states has been proven with full mathematical rigor by Sviridov [12] (see also [13]) for Floquet states with real (continuous) energy, this was done in a somewhat different form than is of interest for the ionization problem. In this context it is desirable to make appear explicitly in the expansion the *discrete* quasienergy HFFT states corresponding to ionization (obeying Gamow-Siegert boundary conditions). The existence of such an expansion is of importance for the assessment of Floquet predictions for intense laser phenomena, e.g., the appearance and disappearance of light-induced states, etc. As this form of expansion does not seem to have been investigated rigorously (see, however, [13]), we shall explore its validity pragmatically, with physical applications in mind. The comparison will be carried out on the populations in bound dressed states. We shall be finding striking agreement between the two theories in a variety of situations, indicating the potential of the multistate approach.

Dressed-state populations have been considered before, starting with the work by Reed, Knight, and Burnett [14] and Law, Su, and Eberly [15]. More recently, the problem was investigated by Sanpera, Su, and Roso-Franco [16] and Vivirito and Knight [17], although not from the point of view of the HFFT [18]. These investigations were made on one-dimensional (1D) model atoms, with either the ''soft'' Coulomb potential (i.e., with the singularity at the origin smoothed out) [14,15] or short-range potentials [16,17].

We shall illustrate our two-stage comparison of the HFFT and WPD on the 1D model with soft Coulomb potential mentioned. This model has proven capable of revealing important physics (e.g., dynamic stabilization [10]), while being simple enough computationally to allow extensive testing.

The paper is organized as follows. In Sec. II we recall the fundamentals of (single-state) HFFT based on the first iteration, as has been used so far, and present its extension to include the second iteration within the theory (developed in the Appendix). Section III contains the extension of the theory to include superpositions of Floquet states. In Sec. IV we discuss the strategy for comparing WPD and HFFT, and the role of the initial condition. The numerical methods used and the atomic model considered are briefly described in Sec. V. In Secs. VI and VII we compare WPD to the two stages of development of the HFFT envisaged. In Sec. VI we discuss the agreement for ionization, in particular adiabatic stabilization, within the context of the first stage. Then, in Sec. VII we discuss the population dynamics in the dressed states within the context of the second stage. We draw conclusions in Sec. VIII.

II. SINGLE-STATE HFFT

The space-translated form of the Schrödinger equation [19] for the 1D case is

$$[\tfrac{1}{2}\mathbf{P}^2+V(x+\alpha(t))]\Psi=i\,\frac{\partial\Psi}{\partial t}, \tag{1}$$

where $V(x)$ is the unperturbed potential; a.u. are used throughout. For monochromatic radiation with constant field amplitude, $\alpha(t)$ can be chosen as

$$\alpha(t)=\alpha_0\,\cos(\omega t+\chi), \tag{2}$$

where χ is an arbitrary phase.

We insert in Eq. (1) the Floquet ansatz

$$\psi(x,t)=e^{-iEt}\sum_{n=-\infty}^{+\infty}\phi_n(x)e^{-in\omega t}. \tag{3}$$

This yields the system of coupled equations for the Floquet components $\phi_n(x)$:

$$[\tfrac{1}{2}\mathbf{P}^2+V_0-(E+n\omega)]\phi_n=-{\sum_m}'V_{n-m}\phi_m. \tag{4}$$

Here $V_n(\alpha_0;x)$ are the Fourier components of $V(x+\alpha(t))$. As $V(x)$ is real and assumed to be even, the V_n are real and we have

$$V_n(-x)=(-1)^nV_n(x),\quad V_{-n}(x)=V_n^*(x)=V_n(x). \tag{5}$$

In Eq. (4) and hereafter, a primed sum Σ' indicates that terms containing V_0 should be omitted. For each solution $\psi(x,t)$, the successive $\phi_n(x)$ have alternating parity: $\phi_n(-x)=(-1)^{n+P}\phi_n(x)$, where $P=0,1$ gives per definition the parity of the solution. For the case in which one-photon ionization is possible (high frequencies), we label the channels such that those with $n\geqslant 1$ are open and those with $n\leqslant 0$ are closed. We impose resonance state (Gamow-Siegert) boundary conditions on the $\phi_n(x)$ (see [5,6]). $E\equiv W-i(\Gamma/2)$ in Eq. (3) represents the ''quasienergy'' of the state, where W is interpreted as its average energy in the field and Γ is its total ionization rate. The Floquet state (3) describes an *ionization mode* consisting of the constant flow of electron population from the vicinity of the nucleus to the asymptotic region, characterized by the quasienergy E and the exponential decay law.

The HFFT proceeds by successive iterations, which give contributions that are of increasing dominant order in ω^{-1}. To *lowest order* (i.e., in the high-frequency limit $\omega\to\infty$ at fixed α_0) the HFFT extracts from Eq. (4) the *atomic structure equation* [5,20]

$$[\tfrac{1}{2}\mathbf{P}^2+V_0(\alpha_0;x)]u=W(\alpha_0)u. \tag{6}$$

With our labeling of the channels, we have to lowest order $\phi_0\cong u(\alpha_0,x)$, where the high-frequency dressed state $u(\alpha_0,x)$ is a solution of Eq. (6); all other $\phi_n\cong 0$. At $\alpha_0=0$, $u(\alpha_0,x)$ goes over into an eigenfunction of the field-free Hamiltonian [with potential $V(x)$]. The eigenvalues $W(\alpha_0)$ are real; hence $E\cong W(\alpha_0)$ and $\Gamma\cong 0$. $W(\alpha_0)$ is inde-

pendent of ω at all α_0. The successive dressed eigenfunctions u of Eq. (6) have alternating parity. It has been shown [5] that at large α_0, an even-odd (gerade-ungerade) degeneracy sets in: The eigenvalues of Eq. (6) coalesce in pairs, one even with one odd, starting with the lowest ones (this occurrence is coupled to the appearance of the ''dichotomy'' effect; see [5]).

The *first iteration* within the HFFT yields for the *total ionization rate* of the state $u(\alpha_0,x)$:

$$\Gamma = 2\pi \sum_{m>0} \sum_{P} |\langle u^P_{k_m}|V_m|u\rangle|^2. \tag{7}$$

Here $u^P_{k_m}(\alpha_0,x)$ are final continuum dressed states, solutions of the structure equation (6); they are assumed to be normalized in the energy scale [21]. The magnitude of the final momenta k_m is determined by the energy conservation equation $(k_m^2/2) = W + m\omega$. The summation over P should be carried out over the parity of the continuum states associated with k_m. Concomitantly with the nonzero value of Γ [Eq. (7)], the first iteration yields non-vanishing expressions for the components $\phi_n(x)$, with $n \neq 0$.

Thus, to lowest orders in ω^{-1}, the HFFT predicts that at high frequencies the atom has a quasistable structure described by the dressed states of Eq. (6). The population in these states decreases exponentially, with rates Γ given by Eq. (7) that are small at high frequencies (see [5], Sec. III B).

However, in the following we shall be needing results for the Floquet components to order ω^{-2}, which are given by the *second iteration* within the HFFT. The second iteration obviously also improves the quasienergy. The general form of the second iteration expressions is derived in the Appendix; see Eqs. (A6)–(A8). If the frequency is sufficiently high, one can use Eqs. (A10) and (A11).

A priori arguments indicate that the HFFT formulas should represent a valid approximation if the following high-frequency condition is satisfied (see [5], Sec. IV D):

$$\omega \gg |\overline{W_0}(\alpha_0)|, \tag{8}$$

where $|\overline{W_0}(\alpha_0)|$ is an average excitation energy of the system. In general, this will be of the order of magnitude of the binding energy of the ground state in the field. Note that Eq. (8) represents a sufficient condition and that in practical cases the validity condition appears to be weaker [6]. We emphasize that there are no restrictions on α_0, as long as condition Eq. (8) is satisfied [22]; this was confirmed recently by calculations on a 1D model [6].

General Floquet theory assumes that the radiation has constant field amplitude. This is not the case when dealing with laser pulses. Nevertheless, if certain conditions are met (see [5], Sec. II A), the theory can be applied by simply ascribing *a posteriori* time dependence to the field amplitude contained in the Floquet state (3). One of these conditions is that the field amplitude variation be slow on the atomic time scale, so that the atom have time to adjust adiabatically to it.

The HFFT as described above, with Gamow-Siegert boundary conditions, applies to ionization. By imposing scattering boundary conditions on the Floquet components ϕ_n, the theory describes the related phenomenon of free-free transitions, i.e. scattering of the electron by the potential, accompanied by multiphoton absorption; see [4(a)]. The latter set of solutions forms a continuum counterpart to the discrete set of quasienergy states.

III. MULTISTATE HFFT

In order to extend the scope of the HFFT, we shall consider now the possibility of representing a wave packet $\Psi(x,t)$, i.e., a square-integrable solution of the time-dependent Schrödinger equation (1), by a superposition of HFFT states Eq. (3). The individual states will be denoted by $\psi^{(\nu)}$ and a superscript (ν) will be attached to the related quantities, e.g., $E^{(\nu)}$. [The state-labeling superscript (ν) introduced here should not be confused with the iteration-labeling superscripts (1) or (2) used in the Appendix.] By definition, for $\omega \to \infty$, $\psi^{(\nu)}$ goes over into the dressed eigenstate of Eq. (6), u_ν, discrete or continuous (for the continuous case the subscript ν stands for $\nu \equiv \{W,P\}$). We write the superposition as

$$\Psi(x,t) = \mathsf{S}_{\nu} C_\nu \psi^{(\nu)}(x,t), \tag{9}$$

with constant coefficients C_ν. The symbol S emphasizes the fact that the summation contains in general discrete and continuous contributions. Note that Eq. (9) will be an exact solution of the Schrödinger equation (1) only if the amplitude α_0 is constant.

The general validity of expansion (9) expresses the *completeness* of the Floquet system of states. This is a delicate mathematical property, which was rigorously proven by Sviridov [12] for the case when the quasienergies are real, i.e., only scattering Floquet states appear in the expansion. The convergence should be understood in the weak sense, i.e., in terms of projections on given functions. In this case the spectrum of the Floquet system (4) is entirely continuous, extending on the real axis from $-\infty$ to $+\infty$ [13]. We are, however, interested in a version of Eq. (9) that brings in explicitly the contribution of the discrete quasienergy states. This could be obtained, in principle, by distorting the integration contour over the continuous spectrum in Eq. (9), from the real energy axis into the complex plane, beyond the singularities of the continuum Floquet states (located at the discrete quasienergies [23]), assuming that the required analyticity conditions are met (see, however, [13]). Application of the residue theorem would then allow one to single out their pole contributions and Eq. (9) would thus contain a discrete sum over quasienergy states plus an integral over a (distorted) continuum. The conditions of validity of an expansion of this type do not seem to have been investigated in the Floquet case, although a similar expansion was proven to exist for wave packets of time-independent Hamiltonians with shape resonances, described in terms of Gamow states [23,24]. We shall explore the possibility of such Floquet expansions in the following numerically, with physical applications in mind.

Whereas the quasienergy states $\psi^{(\nu)}$ repeat themselves identically mod ω, the summation in Eq. (9) should be performed only over states that are distinct. A consistent way to obtain them all, in the high-frequency case, is by identifying them by their $\omega \to \infty$ limit u_ν, as we have done. We can then

use for the discrete quasienergy states $\psi^{(\nu)}$ the second-order expressions given by Eqs. (3), (A10), and (A11).

On the other hand (under conditions well understood), any wave packet $\Psi(x,t)$ can be expanded in the complete set of dressed states $\{u_\mu(x)\}$:

$$\Psi(x,t)=\mathsf{S}_\mu A_\mu(t)u_\mu(x), \tag{10}$$

where S again represents a summation over the discrete spectrum plus an integration over the continuum. The connection between A_μ and C_ν is

$$A_\mu(t)=\mathsf{S}_\nu C_\nu\langle u_\mu|\psi^{(\nu)}\rangle. \tag{11}$$

The integrals representing the scalar products $\langle u_\mu|\psi^{(\nu)}\rangle$ for discrete quasienergy states may not be convergent in general because of the Gamow-Siegert boundary conditions obeyed by $\psi^{(\nu)}$. However, this difficulty has already been taken care of by the procedures of the HFFT for the calculation of $\psi^{(\nu)}$, as shown in the Appendix.

By inserting the second iteration expression of $\psi^{(\nu)}$ [Eqs. (A10) and (A11)] into Eq. (11), we find to $O(\omega^{-2})$

$$A_\mu(t)=\mathsf{S}_\nu T_{\mu\nu}(t)C_\nu, \tag{12}$$

with

$$T_{\mu\nu}(t)=e^{-iE_\nu t}\Bigg\{\delta_{\mu\nu}+\langle u_\mu|G'(E^{(\nu)})\overline{V_1}(E^{(\nu)})|u_\nu\rangle + {\sum_n}' e^{-in\omega t}\Bigg[\langle u_\mu|G(E_n^{(\nu)})V_n|u_\nu\rangle + {\sum_m}' \langle u_\mu|G(W_n^{(\nu)})V_{n-m}G^{(+)}(W_m^{(\nu)})V_m|u_\nu\rangle\Bigg]\Bigg\}, \tag{13}$$

where now we have defined $E_n^{(\nu)}\equiv E^{(\nu)}+n\omega$, with the quasienergy $E^{(\nu)}$ calculated to first order (we recall that this notation deviates from that in the Appendix). Note that the matrix elements appearing in Eq. (13) are well defined if the potentials V_n are regularized according to the HFFT prescription [25].

We shall slightly simplify Eq. (13) by replacing $G(E_n^{(\nu)})$ with its value $G^{(+)}(W_n^{(\nu)})$ at the closely lying point $W_n^{(\nu)}+i\epsilon$ [see the discussion in the Appendix, after Eq. (A7)]. Whereas this has only a minor numerical effect (in view of the agreement achieved in Sec. VII), it avoids the complication of working on the second Riemann sheet. We can express further the coefficients $A_\mu(t)$, using the eigenfunction expansions for the Green's operators involved [e.g., see [5], Eqs. (61) and (64)]:

$$A_\mu(t)=\mathsf{S}_\nu C_\nu e^{-iE_\nu t}\Bigg\{\delta_{\mu\nu}+(1-\delta_{\mu\nu})(W_\nu-W_\mu)^{-1}\times\langle u_\mu|\overline{V_1}(W_\nu)|u_\nu\rangle + {\sum_n}' e^{-in\omega t}(W_\nu+n\omega-W_\mu+i\varepsilon)^{-1}\times\Bigg[\langle u_\mu|V_n|u_\nu\rangle + {\sum_m}' \langle u_\mu|V_{n-m}G_m^{(+)}(W_\nu)V_m|u_\nu\rangle\Bigg]\Bigg\}. \tag{14}$$

Expressions Eqs. (13) and (14) are valid to $O(\omega^{-2})$ included, if one assumes that coefficients C_ν are $O(1)$ constants.

We shall express the initial form of $\Psi(x,t)$ at $t=0$ as

$$\Psi_0=\mathsf{S}_\mu a_\mu u_\mu, \tag{15}$$

where $a_\mu\equiv A_\mu(0)$. By comparing with Eq. (12),

$$a_\mu=\mathsf{S}_\nu T_{\mu\nu}(0)C_\nu. \tag{16}$$

This linear relation allows the determination of the C_ν from the a_μ, assumed known.

IV. WAVE-PACKET DYNAMICS

In the WPD approach, the time-dependent Schrödinger equation is integrated numerically starting from a square-integrable initial condition. Usually, the initial condition is taken to be a field-free energy eigenstate of the atom. The laser pulse is applied and the wave packet is propagated in time until the pulse is turned off. Ionization probabilities are calculated at the end of the pulse according to the quantum-mechanical laws, from the projections of the wave packet (in the laboratory frame) onto the field-free continuum states of the atom. Under these conditions, the ionization probabilities found describe global atomic behavior, depend on the shape of the pulse, and therefore are not characteristic quantities of the initial atomic state [14], [11], [17]. In particular, if the laser field has a large peak value and is turned on rapidly (over a few cycles), it applies a sudden shock to the atom, so that the population is projected to higher discrete states, or to the continuum (atomic ''shake-up''), from the very beginning; it will be in these states that the population will evolve during the rest of the pulse and not in the ground state.

In contrast to the fully realistic approach of WPD, Floquet theory, as well as the HFFT, operates with the individual idealized states (3). The disparity of the operating assumptions of the two theories is a handicap for their comparison. The correct choice of the initial condition for WPD is therefore essential. For consistency, this should be taken not as a field-free atomic state but rather as a state that describes the atom already in the stationary regime imposed by a high-frequency field of constant amplitude. States representing this kind of situation are the high-frequency bound dressed states u_μ, close approximations to the HFFT states $\psi^{(\mu)}$ [26]. In fact, in the stationary approach, $\psi^{(\mu)}$ describes precisely the ionization mode, characterized by the quasienergy $E^{(\mu)}$, consisting of the transfer of population from the bound dressed state u_μ (confined to the vicinity of the nucleus) towards the asymptotic region. In this language, the signature of the ionization can be viewed as the time decrease of the ''survival probability'' $P_\mu(t)=|\langle u_\mu(x)|\Psi(x,t)\rangle|^2$.

As mentioned in the Introduction, we shall make the comparison of the theories in two stages. In the first stage, we shall apply WPD to the case of an atom initially in the dressed ground state $u_0(x)$ and follow the subsequent evolution of its population to check if it is indeed given by an exponential decay law $\exp(-\Gamma t)$, as predicted by the single-

state HFFT (and by general single-state Floquet theory). In the process, we shall compare the decay rates from the two theories, which will enable us to ascertain if WPD confirms the existence of adiabatic stabilization (see Sec. VI).

One can anticipate, however, that the agreement of the two theories will be necessarily handicapped by shortcomings of the current form of the HFFT. These can be ascribed to two independent causes. (a) The use of the first iteration in ω^{-1} of the HFFT has limited accuracy at finite ω, and higher approximations within the HFFT may be needed. (b) At finite ω the dressed state used as initial condition is not an exact solution of Eq. (1), as is the Floquet state it approximates. Due to this mismatch, the wave packet cannot be expected to coincide with a single Floquet state.

In the second stage of the comparison of the theories, we shall try to overcome these deficiencies. To surpass (a), we shall include in our calculation the second-order iteration within the HFFT, developed in the Appendix. We conjecture that (b) can be transcended by introducing a *multistate HFFT* description for the wave packet, of the form Eq. (9), which includes discrete quasienergy states. In fact, we shall focus here on the case when the contribution of the discrete spectrum is dominant and the continuum contribution can be neglected (physically, discrete excitations dominate the continuum ones). One may expect that this will be the case if the initial condition (15) contains only energetically low-lying dressed states. The coefficients C_ν of the expansion (9) will be determined via the HFFT with the help of the initial condition (15), as shown in Sec. VII.

We shall test the agreement of the multistate HFFT with WPD on the evolution of the populations $P_\mu(t)$ in bound dressed states during ionization. We shall limit ourselves to the projections on bound states. For WPD the $P_\mu(t)$ are obtained by projecting the numerically integrated wave packet $\Psi(x,t)$ onto the bound dressed states; for the multistate HFFT they are given by $P_\mu(t)=|A_\mu(t)|^2$ with the $A_\mu(t)$ from Eq. (14). For the purpose of the comparison, the $P_\mu(t)$ can be regarded as merely mathematical tools, independently of their physical significance.

V. ATOMIC MODEL: NUMERICAL METHODS

We shall illustrate the general ideas of the previous sections on the case of a *1D atomic model* having as field-free potential the soft Coulomb potential

$$V(x)=-\frac{1}{(1+x^2)^{1/2}}, \tag{17}$$

which has been frequently used in the past; see e.g., [27,10]. $V(x)$ has a Coulomb tail and therefore supports a Rydberg series of energy levels. The Coulomb singularity at the origin has been ''softened,'' so that there exists a ground state with even parity; its energy is $W_0=-0.67$.

Let us now make a few comments on the *numerical methods for the HFFT calculation*. The eigenvalues of the HFFT structure equation (6), corresponding to the potential $V(x)$ of Eq. (17), although calculated many times, will be reproduced in Fig. 1 for reference. The successive levels of the even states will be labeled by $n=0,2,...$ those for the odd states by $n=1,3,...$. The level coalescence mentioned in Sec. II is apparent in Fig. 1 for the $n=0$ and 1 states; for the $n=2$ and 3 states it barely starts at $\alpha_0=15$.

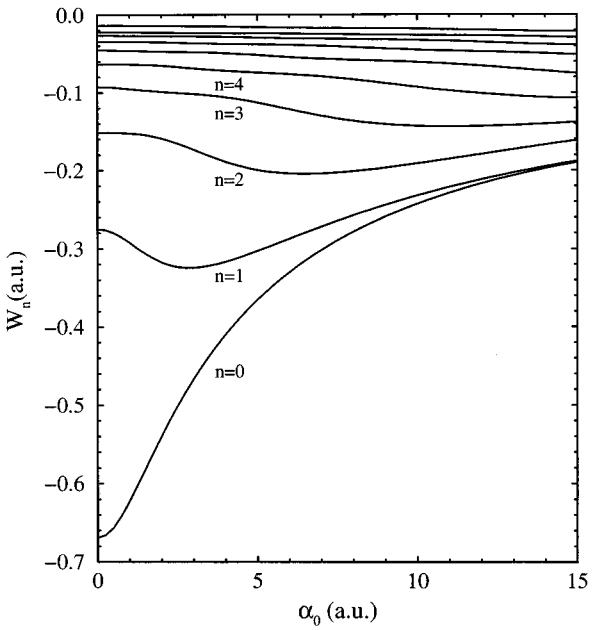

FIG. 1. Dressed energy levels of the high-frequency structure equation (6) with the soft Coulomb potential (17).

The other quantities required by the HFFT calculation, such as the widths Γ of Eq. (7) and the amplitudes $A_\mu(t)$ of Eq. (14), have been computed using the methods described by Marinescu and Gavrila [6]. For example, in the expression of $A_\mu(t)$, we have the recurrent matrix element

$$\begin{aligned}\langle u_\mu|\overline{V_1}(W_\nu)|u_\nu\rangle &\equiv \sum_n{}' \langle u_\mu|V_n G^{(+)}(W_\nu+n\omega)V_n|u_\nu\rangle \\ &= \sum_n{}' \langle u_\mu|V_n|\chi_{k_{n\nu}}\rangle \\ &\quad - i\pi\sum_{n>0}\sum_P \langle u_\mu|V_n|u^P_{k_{n\nu}}\rangle\langle u^P_{k_{n\nu}}|V_n|u_\nu\rangle.\end{aligned} \tag{18}$$

We have made use here of Eq. (A4) and have defined

$$|\chi_{k_{n\nu}}\rangle \equiv \mathrm{P}[(W_\nu+n\omega-H)^{-1}]V_n|u_\nu\rangle, \tag{19}$$

where P is the principle value operator and

$$\tfrac{1}{2}k^2_{n\nu}\equiv W_\nu+n\omega. \tag{20}$$

Equation (18) is thereby similar to the ones encountered in [6]; for the calculation of $|\chi_{k_{n\nu}}\rangle$ [Eq. (19)], we have applied the Dalgarno-Lewis method [28]. Unlike in [6], however, where a short-range potential was used, here we had to face the difficulty of the long tail of the soft Coulomb potential. This was done using known asymptotic-expansion procedures (e.g., see [29]).

We now comment on our *numerical methods for the WPD calculation*. We solve the space-translated Schrödinger equation (1) using lattice techniques to obtain a discrete representation of the wave function, i.e., $\psi(x)\Rightarrow\psi(x_i)\equiv\psi_i$, and of

all coordinate-space operators on a one-dimensional mesh. Local operators such as potentials simply become diagonal matrices of their values at lattice points, i.e., $V(x) \Rightarrow V_i \delta_{ij}$. Derivative operators, such as the kinetic energy, have lattice representations in terms of matrices, i.e., $\partial/\partial x \Rightarrow D_{ij}^{(x)}$. In particular, we use here the Fourier-collocation method [30] for the kinetic-energy operator. As a result, all calculations discussed here implement uniform-mesh spacing.

Because of its efficiency, we apply the Fourier-collocation method using the fast Fourier transform to evaluate the action of the lattice kinetic-energy operator in momentum space, where it is diagonal. If only a few low-lying states are desired, as is our case, these may be obtained efficiently using iterative methods, such as the Lanczos algorithm for partial eigensolutions of the Hamiltonian [31]. The eigenvectors are used as initial conditions for the time evolution and for computing the time-dependent population of the wave packet in a given dressed eigenstate.

The formal solution of the time-dependent Schrödinger equation is

$$\psi_j(t) = U(t,t_0)\psi_j(t_0), \tag{21}$$

where we have omitted the spatial coordinates for simplicity and the evolution operator $U(t,t_0)$ is given by the time-ordered exponential

$$U(t,t_0) = \mathcal{T} \exp\left\{ -i \int_{t_0}^{t} H(t')dt' \right\}. \tag{22}$$

We discretize time in the sense that the electromagnetic interaction is taken as constant in successive small intervals $\Delta t_k = t_k - t_{k-1}$ $(k=1,2,...,K)$ and express the evolution operator in successive infinitesimal factors

$$U(t,t_0) = U(t,t_{K-1})U(t_{K-1},t_{K-2})\cdots U(t_1,t_0). \tag{23}$$

In this case the time ordering can be ignored.

Two methods have been employed to approximate the infinitesimal time-evolution operator [32]

$$U(t_k,t_{k-1}) = \exp\{-iH(t_k)\Delta t_k\}, \tag{24}$$

a Taylor series expansion of L terms, where L is chosen at each step according to a convergence criterion on the wave function (see [31]), and the symmetric split-operator propagator of Feit, Fleck, and Steiger [33]. The split operator is explicitly unitary by construction and is accurate to order $(\Delta t)^2$. The Taylor-series expansion is not explicitly unitary, but in practice the norm of the wave function can be conserved to high precision.

VI. IONIZATION RATES: ADIABATIC STABILIZATION

In this section we study ionization rates and compare the results of WPD with those of the first iteration within the single-state HFFT. We choose the frequencies $\omega = 2$ and 4, which are, respectively, about three and six times larger than the binding energy of the field-free atom, and allow α_0 to vary from 0 to 20. According to the criterion (8), the frequencies are well suited for comparison with the HFFT, particularly at larger α_0 (see Fig. 1). We take as an initial condition for the wave packet the dressed ground state. Figure 2 gives the evolution of its population $P_0(t)$ for three α_0. The curves shown have a rather smooth decay, but display increasing jitter as α_0 increases [note the change of scale in the ordinate of Fig. 2(b)]. However, for $\alpha_0 = 20$ (not shown), the jitter has practically disappeared.

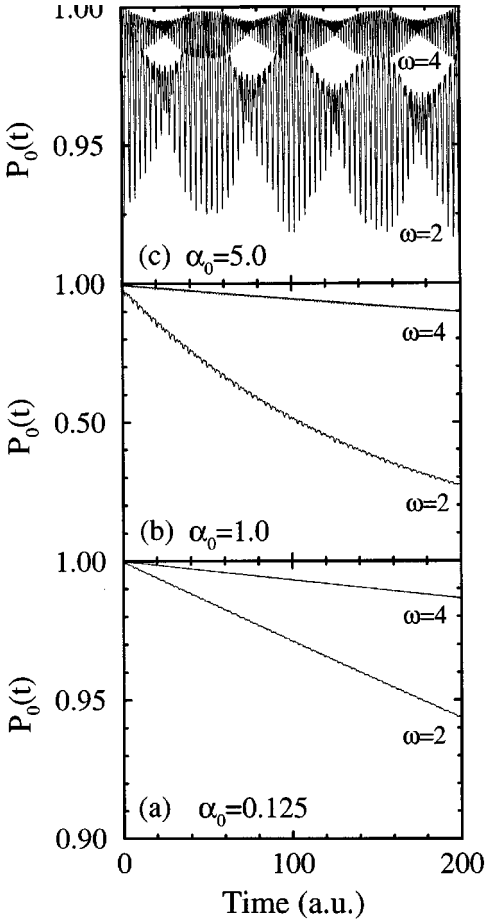

FIG. 2. Time dependence of the population $P_0(t)$ in the dressed ground state for a wave packet evolving from this state at two high frequencies ω and three α_0 (in a.u.). The field is described by Eq. (2), with $\chi = -(\pi/2)$.

The curves for $\alpha_0 = 0.125$, 1, 20, can be fitted quite accurately to decaying exponentials $\exp(-\Gamma t)$. Even for $\alpha_0 = 5$, the *average* population is rendered quite well by a decaying exponential. To increase the accuracy, the values of Γ were extracted by following the evolution of $P_0(t)$ as long as possible, over thousands of cycles in some cases [34].

These facts confirm qualitatively the single-state HFFT, which predicts exponential decay for the populations when the validity criterion (8) is satisfied. The agreement does improve with increasing α_0, as predicted, and for the higher frequency $\omega = 4$ the decay is considerably slower than for $\omega = 2$, also as predicted. Concerning the jitter superposed on the exponential decay, this is due to the coupling of the ground state to excited states and cannot be accounted for by a single-state HFFT description. The situation will be analyzed in detail in Sec. VII.

We mention that the exponential decay of the dressed-state populations in the stabilization regime has been studied earlier with WPD for a 1D model with a $\delta(x)$ potential by Sanpera, Su, and Roso-Franco [16]. Rates were extracted,

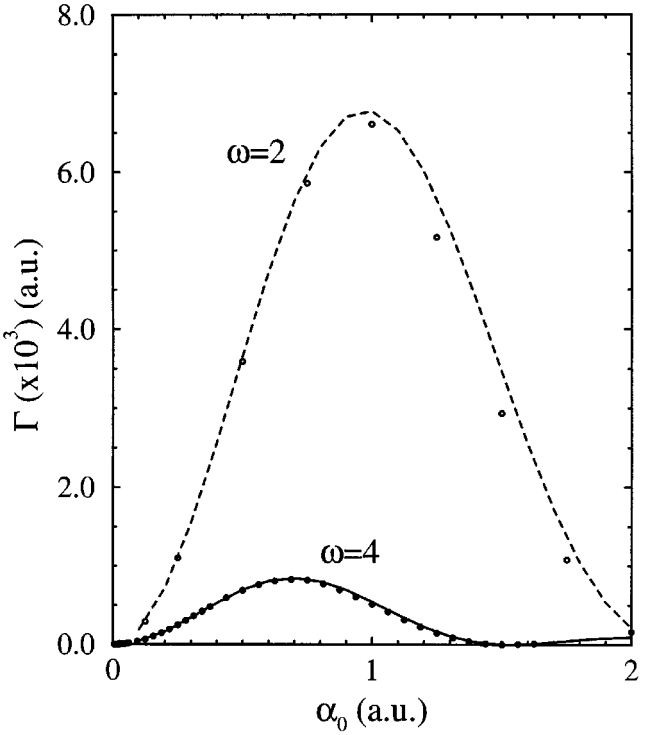

FIG. 3. Ionization rate Γ of the dressed ground state for a restricted range α_0 and two high frequencies ω (in a.u.). Wave-packet dynamics (WPD) results, open and closed circles; high-frequency Floquet theory (HFFT) results, dashed and full curves. The ascending branches of the curves correspond to perturbation theory, the descending branches to the adiabatic stabilization regime.

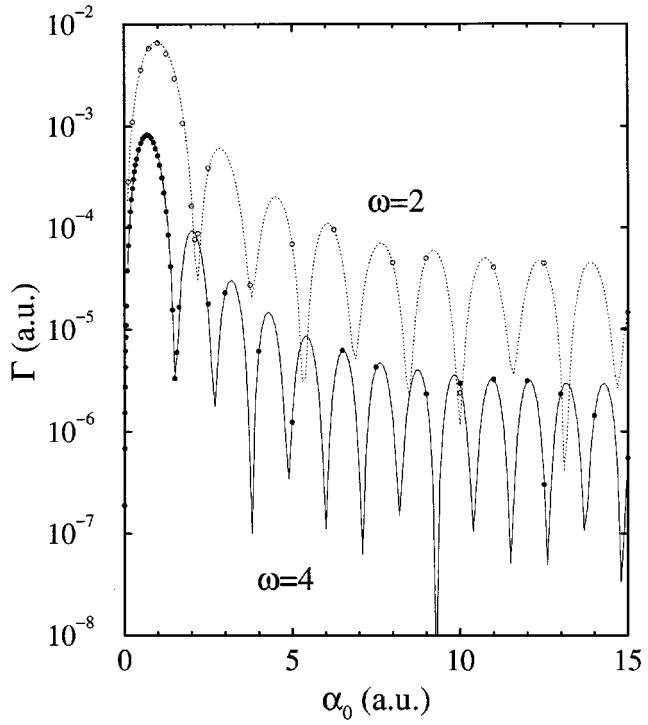

FIG. 4. Ionization rate Γ of the dressed ground state for an extended range α_0 and two high frequencies ω (in a.u.), according to WPD (open and closed circles) and the HFFT (dotted and full curves). Concerning the oscillatory behavior of Γ in the stabilization regime, see [35,6].

but no reliable results from HFFT were available for comparison.

The values of Γ thus obtained from WPD are collected in Fig. 3 for $0<\alpha_0<2$ and in Fig. 4 for the extended interval $0<\alpha_0<15$; in the latter case a logarithmic scale is needed. In the same figures we present also the results from the first-order iteration of the HFFT, Eq. (7). As apparent, the WPD results are in good quantitative agreement with those of the HFFT, particularly at $\omega=4$. The agreement extends over a large α_0 range and four orders of magnitude of Γ, as seen in Fig. 4.

These figures display the phenomenon of *adiabatic stabilization*; see [5], Sec. VI. Following a parabolic increase at small α_0, as predicted by perturbation theory [35], Γ passes a maximum around $\alpha_0=1$ and then *decreases* to zero at larger α_0, albeit in an oscillatory manner. We have thus demonstrated that adiabatic stabilization results also from WPD, if the initial condition is adequately chosen, and has the features predicted by the HFFT.

The oscillatory behavior of Γ beyond its maximum has been encountered also for short-range (Gaussian) 1D potential models [36,6]. It contrasts with the monotonically decreasing behavior (albeit with slight undulations) existing in the 3D Coulomb case [9(a)]. It was concluded in [6] that the oscillations are a specific feature of 1D models.

To end this section we note that the discrepancies found between WPD and HFFT can be traced back to those anticipated in Sec. IV, referred to as (a) and (b). We shall try to remedy them in the next section.

VII. POPULATION DYNAMICS

We have studied the dynamics of the populations in dressed states for two kinds of *initial conditions*, one (i) containing only the ground state, the other (ii) in which several low-lying bound states are present. Case (ii) represents a rather general situation. Indeed, when in WPD the field is turned on rapidly upon an unperturbed atom, the population is projected out of the ground state into excited states (shake-up). After the peak of constant intensity has been reached at time τ, an analysis of the wave packet in terms of dressed states shows that discrete as well as continuum states may be populated (e.g., see [14,15,11]). However, if the shake-up is not too violent, most of the population will be found in lower-lying bound states. By taking the situation at time τ as the initial condition for the subsequent evolution of the wave packet, case (ii) emerges.

In case (i) we take $a_0=1$ and $a_{\mu\neq 0}=0$ in Eq. (15). We illustrate case (ii) by taking $a_0=a_1=a_2=1/\sqrt{3}$, with all other a_μ vanishing. The field parameters were taken $\omega=2$ and $\alpha_0=5$ in all cases. From Fig. 1 one gets a ratio of photon energy to ground-state binding energy of approximately 5, so that the high-frequency criterion (8) is reasonably well satisfied. Further, we have given two values to the phase χ in Eq. (2), $\chi=0$ and $-(\pi/2)$, which represent, from the WPD and multistate HFFT points of view, two different physical situations. The physical results of the single-state HFFT are, of course, independent of χ.

We shall now elaborate on the calculation of the populations P_μ according to the multistate HFFT. In order to determine the coefficients $A_\mu(t)$ [Eq. (14)], the first step is to

calculate the coefficients C_ν from Eq. (16). We have restricted our initial conditions to contain only a few low-lying dressed states u_μ, i.e., with only a few nonvanishing a_μ (for, say, $\mu \leqslant M$) in Eq. (15). We may assume, therefore, that only low-lying HFFT states $\psi^{(\nu)}$ with $\nu \leqslant N$ will be needed in Eq. (9); N is chosen large enough as to ensure convergence of the final results (obviously, $N > M$). (In practice, in the following calculations, N was taken to be 10.) By restricting also the coefficients a_μ by the condition $\mu \leqslant N$ (setting, obviously, those for $\mu > M$ equal to zero), the matrix $T_{\mu\nu}(0)$ in Eq. (16) becomes square. As it is also nonsingular [37], this allows the unique determination of the coefficients C_ν, either numerically or analytically (as expansions in ω^{-1}). We note that for $\omega^{-1} \to 0$ we have $T_{\mu\nu}(0) = \delta_{\mu\nu}$ and $C_\nu = a_\nu$. Therefore, at nonvanishing ω^{-1}, $C_\sigma = O(1)$ for $\sigma \leqslant M$, while for $\tau > M$, C_τ must be $O(\omega^{-1})$ or higher. In fact, calculations show that the order of magnitude of C_τ depends on the phase χ of the field (2): If $\chi \neq 0$, C_τ is effectively $O(\omega^{-1})$, but for $\chi = 0$, it is of higher order. Considering then Eq. (14), we infer that for $\sigma \leqslant M$ we have $A_\sigma = O(1)$, whereas for $\tau > M$, A_τ must be $O(\omega^{-1})$ or higher. Thus $|A_\sigma|^2 = O(1)$ and $|A_\tau|^2 = O(\omega^{-2})$. This means that only the lowest nonvanishing order in the calculation of A_τ is relevant for consistency to order ω^{-2}.

In case (i) we find from Eq. (14), by consistently extracting the dominant terms in ω^{-1} with the help of Eq. (8), the analytic result

$$A_0(t) = C_0 e^{-iE_0 t}\left\{1 + \sum_n{}' \frac{e^{-in\omega t}}{n\omega}\left[\langle u_0|V_n|u_0\rangle + \sum_m{}' \frac{1}{m\omega}\langle u_0|V_{n-m}V_m|u_0\rangle\right]\right\} + \sum_{\nu>0}\sum_n{}' C_\nu e^{-iE_\nu t}\frac{1}{n\omega}\langle u_0|V_n|u_\nu\rangle, \tag{25}$$

$$A_\tau(t) = C_\tau e^{-iE_\tau t} + C_0 e^{-iE_0 t}\sum_n{}' e^{-in\omega t}\frac{1}{n\omega}\langle u_\tau|V_n|u_0\rangle \quad (\tau \neq 0). \tag{26}$$

These expressions were written, taking into account the order of magnitude of the C_ν, such that $A_0(t)$ be valid to $O(\omega^{-2})$ included, and $A_\tau(t)$ be valid to $O(\omega^{-1})$. The disparity in the two orders stems from the fact that we are interested in obtaining correct expressions to $O(\omega^{-2})$ for all populations $P_\mu(t)$. Because of Eq. (5) and the fact that the functions u_τ are real, the sum over n in Eq. (26) is purely imaginary. Thus

$$|A_\tau(t)|^2 = |C_\tau|^2 e^{-\Gamma_\tau t} + \frac{1}{\omega^2}|C_0|^2 e^{-\Gamma_0 t}\left|\sum_n{}' e^{-in\omega t}\frac{1}{n}\langle u_\tau|V_n|u_0\rangle\right|^2 - \frac{4}{\omega}|C_\tau C_0| e^{-(\Gamma_\tau+\Gamma_0)t/2}\sin[(W_\tau - W_0)t + \arg(C_\tau^* C_0)]\,\mathrm{Im}\sum_{n>0} e^{-in\omega t}\frac{1}{n}\langle u_\tau|V_n|u_0\rangle \quad (\tau \neq 0). \tag{27}$$

The expression of $|A_0(t)|^2$ is similar and will not be given here. Note that the individual populations have an oscillatory behavior with the field frequency ω and its harmonics. Moreover, the last term in Eq. (27) displays *beats* on top of the field oscillations, with a frequency $W_\tau - W_0$ corresponding to the transition between the initially populated and the final dressed state considered.

The existence of beats in the dressed-state populations has been signaled, under similar initial conditions, by Vivirito and Knight [17]. They used a two-state model (with no continuum) combined with perturbation theory to explain qualitatively their occurrence. In our case, they appear as a direct consequence of the dominance of the states $n = 0,1$ in the Floquet expansion (9), with no adjustments needed.

If one adds up the populations in *all* bound states, one finds to $O(\omega^{-2})$

$$\sum_n P_n(t) = \sum_n |C_n|^2 e^{-\Gamma_n t} + \frac{1}{\omega^2}|C_0|^2 e^{-\Gamma_0 t}\sum_m{}'\left\{\frac{1}{m^2}\langle u_0|V_{-m}Q_b V_m|u_0\rangle + \sum_{k\neq 0,m} e^{-ik\omega t}\frac{1}{m(k-m)}\langle u_0|V_{k-m}Q_c V_m|u_0\rangle\right\}. \tag{28}$$

Here Q_b and Q_c are the projectors on all bound, and all continuum states, respectively ($Q_b + Q_c = I$). The beat terms $O(\omega^{-2})$ contained in the individual populations with $n \neq 0$ [see Eq. (27)] have canceled out against those existing in $P_0(t)$. Equation (28) still contains oscillatory terms (sum over k in the curly bracket), but these are numerically much smaller than those giving the jitter in the individual populations, because the matrix elements of the former contain an extra Q_c sandwiched between bound states. The rest of the terms in Eq. (28) have a smooth exponential decrease in time.

The analytic result for case (ii) can be derived similarly. From Eq. (14), for $\mu \leqslant M$ we find

$$A_\mu(t) = C_\mu e^{-iE_\mu t}\left[1 + \sum_n{}' e^{-in\omega t}\frac{1}{n\omega}\langle u_\mu|V_n|u_\mu\rangle\right] + \sum_{\sigma=0}^{M}(1-\delta_{\sigma\mu})C_\sigma e^{-iE_\sigma t} \times \sum_n{}' e^{-in\omega t}\frac{1}{n\omega}\langle u_\mu|V_n|u_\sigma\rangle. \tag{29}$$

This expression is $O(1)$, and is given here to $O(\omega^{-1})$ included. The corresponding populations $P_\mu(t)$ contain oscillatory terms of $O(\omega^{-1})$ and display beatlike oscillations. The amplitudes $A_\mu(t)$ for $\mu > M$ are $O(\omega^{-1})$, and will not be given here; the corresponding populations $P_\mu(t)$ are therefore $O(\omega^{-2})$. By adding up the populations in the initially populated states $\mu \leqslant M$ one finds

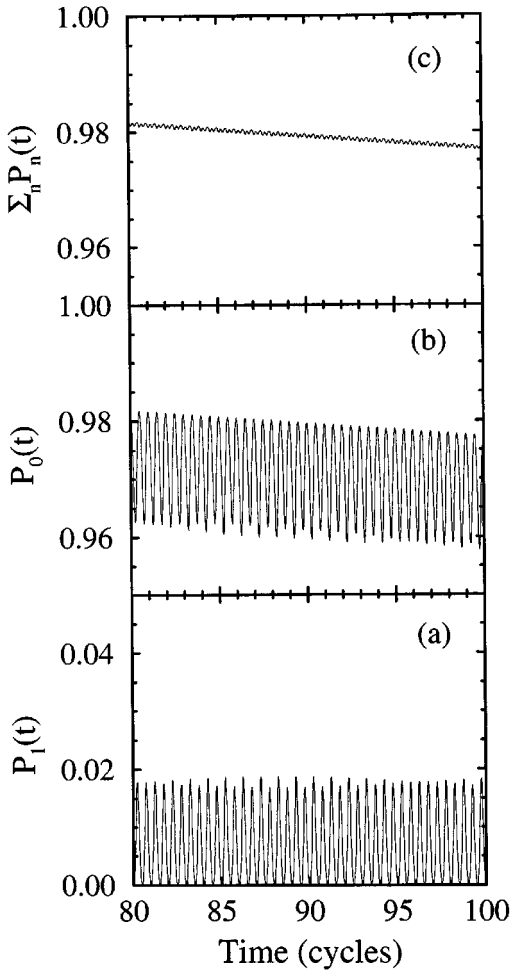

FIG. 5. Populations in the first two dressed states $n=0,1$ of a wave packet evolving from the ground state, at $\omega=2$ and $\alpha_0=5$ (a.u.), in a field given by Eq. (2) with $\chi=0$. The sum ΣP_n represents the population in all bound states. The curves represent the coincident results of WPD and HFFT. Note the cancellation of the oscillations of P_0 and P_1 in ΣP_n.

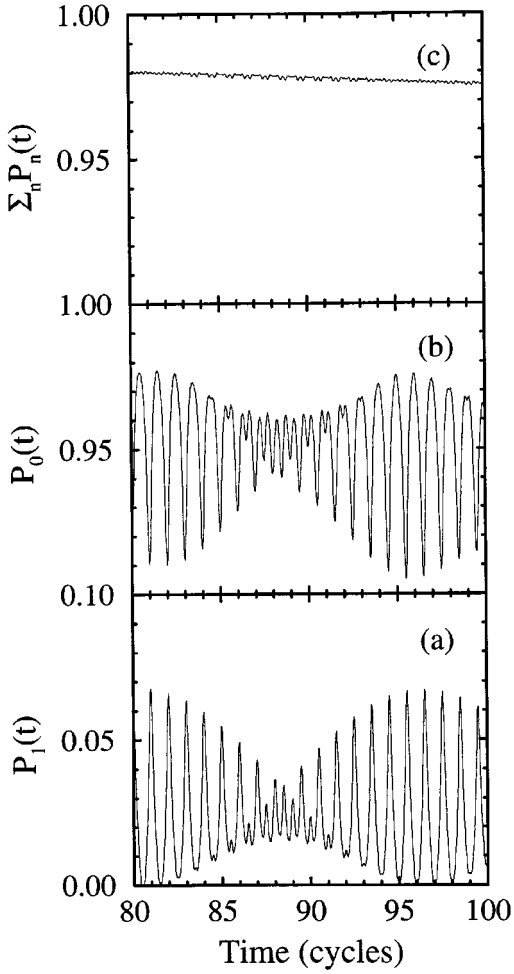

FIG. 6. Populations in the first two dressed states $n=0,1$ of a wave packet evolving from the ground dressed state, at $\omega=2$ and $\alpha_0=5$ (a.u.), in a field given by Eq. (2) with $\chi=-(\pi/2)$. The sum ΣP_n represents the population in all bound states. The curves represent the coincident results of WPD and HFFT. Note the oscillations and beats in P_0 and P_1 and their cancellation in ΣP_n.

$$\sum_{\mu=0}^{M} P_\mu(t)=\sum_{\mu=0}^{M} |C_\mu|^2 e^{-\Gamma_\mu t}+O(\omega^{-2}). \tag{30}$$

In this sum, the oscillatory terms $O(\omega^{-1})$ contained in the individual populations $P_\mu(t)$ have canceled, and we are left with smoothly time-decreasing exponentials. The corrective $O(\omega^{-2})$ terms of Eq. (30) introduce a small jitter. This will be also the case when considering the sum of populations P_μ in *all* bound states to $O(\omega^{-2})$ included.

We now address the issue of the *agreement of WPD and the multistate HFFT*, taking the populations $P_\mu(t)$ as a test case. Beginning with case (i), the $P_\mu(t)$ for the alternative $\chi=0$ are given in Fig. 5, and those for $\chi=-(\pi/2)$ in Fig. 6. We show the populations in the ground state $n=0$, in the first excited state $n=1$, and the sum of the populations in all bound states ΣP_n. A striking fact is that the figures contain the results of both WPD and HFFT, i.e., the results of the two theories coincide within the accuracy of the graphical representation in all fine details. We have chosen to represent the populations starting with the 80th cycle in order to stress that the agreement has not deteriorated in the meanwhile. The results for case (ii) are given in Fig. 7 for $\chi=-(\pi/2)$. The populations for the initially present states $n=0,1,2$ are shown; the sum ΣP_n is given in two versions, one for $0\leqslant\mu\leqslant 2$, the other for all bound μ. The two theories are still indistinguishable for the $n=0$ and 1 populations, but slight discrepancies become visible for the state $n=2$ (WPD, dotted line; HFFT, full line). Even in the latter case the difference amounts to less than 0.1%.

From this and other similar cases analyzed, we conclude that the two theories agree strikingly well when dealing with initial conditions involving low-lying dressed states. This implicitly confirms the multistate HFFT description and checks both numerical computations.

We next focus attention on the *interpretation of the results*. In case (i), only the first excited state ($n=1$, odd) carries significant population (about 2% of the total; see Figs. 5 and 6) in addition to the ground state $n=0$. The population in higher states is quite small, but was included in the sum ΣP_n, given in Figs. 5(c) and 6(c). Thus only the states $n=0$ and 1 are involved in the population flopping during the

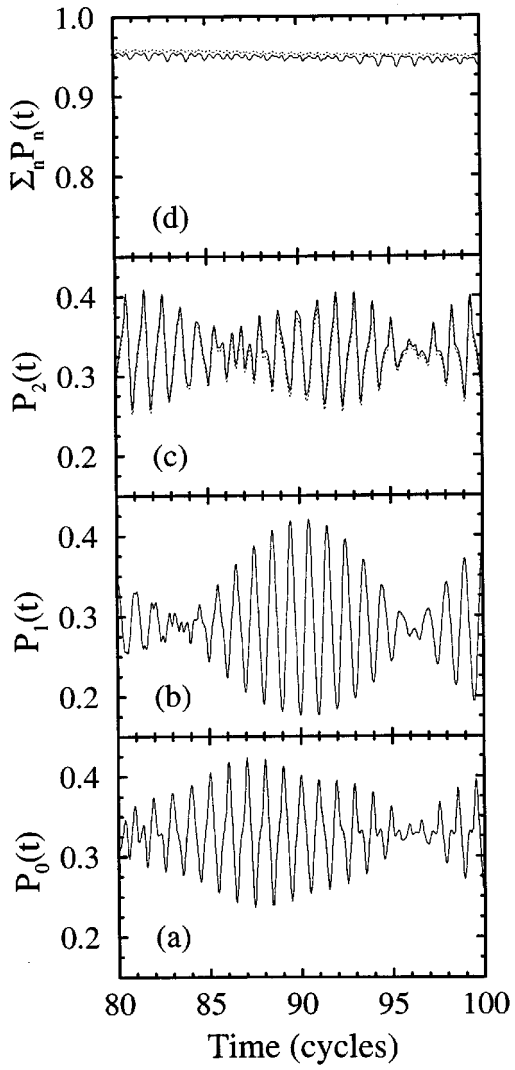

FIG. 7. Populations in the first three dressed states $n=0,1,2$ of a wave packet evolving from a superposition of these states [see case (ii), Sec. VII], at $\omega=2$ and $\alpha_0=5$ a.u., in a field given by Eq. (2) with $\chi=-(\pi/2)$. The results of the WPD and the HFFT are coincident for $n=0$ and 1, but differ slightly for $n=2$ (WPD, dotted curve; HFFT, full curve). Note the beats in the populations. ΣP_n represents the sum of the populations in states $n=0,1,2$ (full line) and in all dressed states (dotted line). Note the nearly complete cancellation of the oscillations in P_0, P_1, P_2 in their sum.

ionization process. There is a significant difference between the way this occurs in the alternatives $\chi=0$ (Fig. 5) and $\chi=-(\pi/2)$ (Fig. 6). The latter shows manifestly beats, whereas the former does not. These are apparent also in Fig. 2 ($\alpha_0=5$, and $\omega=2$ and 4), which refers to the case $\chi=-(\pi/2)$ too. Their existence or nonexistence follows from Eqs. (26) and (27). Indeed, if $\chi=0$, as already mentioned, C_τ is higher than $O(\omega^{-1})$ and hence the first term in Eq. (26) is negligible with respect to the second, with the consequence that Eq. (27) displays an oscillatory behavior, but no beats. If, on the other hand, $\chi\neq 0$, C_τ is $O(\omega^{-1})$, the two terms in Eq. (26) are of the same order of magnitude, and the beats are indeed present in Eq. (27). The frequency of the beats is obviously independent of ω; this is illustrated by Fig. 2(c) for the two cases $\omega=2,4$. It coincides with the atomic transition frequency from $n=0$ to 1, as shown by Eq. (27). The sums over all populations ΣP_n, given in Figs. 5(c) and 6(c), shows practically no jitter, as discussed in connection with Eq. (28).

Turning to case (ii), Fig. 7 for $\chi=-(\pi/2)$ displays beats. (Their presence in a several-state superposition of dressed states was also signaled by Law, Su, and Eberly [15]). Here it is a general feature, independent of χ, because all coefficients C_μ in Eq. (29) are $O(1)$. The sum of the populations in the initially represented states has indeed no oscillations or beats, as predicted by Eq. (30), but does have a jitter representing the $O(\omega^{-2})$ corrective terms in Eq. (30). The addition of the other populations in dressed states increases little the sum, but decreases the jitter level to a few tenths of a percent. Hence, in case (ii) as opposed to case (i), the population trading occurs among the initially populated states, with negligible contribution from the others. In both cases, however, the populations in all bound states decays rather smoothly in time, corresponding to the steady transfer of population to the continuum due to ionization.

VIII. CONCLUSION

In this paper we have assessed the potential of the HFFT in comparison to WPD. As a test ground for the comparison we have used the well-known 1D potential model with soft Coulomb potential, although the conclusions apply, undoubtedly, more generally.

The analysis was carried out in two stages at two levels of accuracy within the HFFT. In the first stage, we have used its current (single-state) form, valid to first order in ω^{-1}. To make the comparison meaningful, we have expressed the initial condition used for the WPD in terms of dressed states, which play a structural role in the HFFT. We have shown that the survival probability in the initial ground dressed state at a given α_0 value follows the exponential law of decay, with a rate that is in good agreement with that given by the HFFT, provided the frequency is large enough. Since the HFFT rate manifests *adiabatic* stabilization, we have thus shown that this results from WPD too, and not only the already known *dynamic* form.

For an improved agreement with WPD, in the second stage of our comparison we have extended the HFFT in two directions: we have included the second-order corrections in ω^{-1} within the theory, and we have introduced the *multistate HFFT*, i.e., the representation of wave packets as superpositions of HFFT states; see Eq. (9). The second extension is based on the mathematical completeness for Floquet states. Although rigorous mathematical proofs guarantee this property for the case of Floquet states with real quasienergy, we have been interested here in the case more adapted to ionization, when the expansion includes discrete quasienergy states. We have considered the case when the initial condition is expressible as a superposition of a number of bound dressed states, which in practice is a rather general situation. We have then compared the predictions of WPD and HFFT for the time evolution of the populations in bound dressed states. In the cases considered, the agreement was remarkable, thus implicitly confirming the potential of the multistate HFFT and our operational assumptions. However, more remains to be done in order to assess the power of the method

and, in particular, the importance of the continuum in the expansion (9).

From a dynamic point of view, our results have shown that there is considerable population flopping between dressed states during the ionization, the characteristics of which are different for one- and several-state initial conditions. As opposed to this, we have shown analytically (with the multistate HFFT) and confirmed numerically (with WPD) that the *sum* of the populations in all dressed bound states undergoes a smooth decay in time.

ACKNOWLEDGMENTS

The work of J.C.W. was supported by the NSF through the Institute for Theoretical Atomic and Molecular Physics. I.S. would like to thank A. Dalgarno for having made possible his participation in the project. M.G. acknowledges partial support from the EC Network ''Atoms in Superintense Laser Fields'' and from the IR Foundation.

APPENDIX: SECOND ITERATION WITHIN THE HFFT

We develop here the second-order iteration within the HFFT from the general formulas derived by Gavrila in [5], Sec. IV B. To this order, Eqs. (81) and (82) of [5] become

$$[H+\overline{V_1}(E^{(2)})+\overline{V_2}(E^{(2)})-E^{(2)}]\phi_0^{(2)}=0, \tag{A1}$$

$$\phi_n^{(2)}=G(E_n^{(2)})\left[V_n+\sum_m{}' V_{n-m}G(E_m^{(2)})V_m(x)\right]\phi_0^{(2)} \quad (n\neq 0). \tag{A2}$$

Here H is the dressed Hamiltonian entering Eq. (6) and $G(E)$ is the Green's operator associated with it. We are using the notation

$$E_n\equiv E+n\omega. \tag{A3}$$

We have also denoted in Eq. (A1),

$$\overline{V_1}(E)\equiv\sum_m{}' V_{-n}G(E_n)V_n, \tag{A4}$$

$$\overline{V_2}(E)\equiv\sum_n{}'\sum_m{}' V_{-n}G(E_n)V_{n-m}G(E_m)V_m. \tag{A5}$$

Superscript (2) in Eqs. (A1) and (A2) labels the values of E and ϕ_n of the second iteration. The order of magnitude of the terms is characterized by the number of ω-dependent Green's functions $G(E_n)$ they contain, because $G(E_n)\sim I(n\omega)^{-1}$, for $\omega\to\infty$.

The Gamow-Siegert boundary conditions on the components ϕ_n require that for open channels ($n\geqslant 1$, $\mathrm{Re}E_n>0$) these should have an oscillatory exponential increase in the asymptotic region, and for closed channels ($n\leqslant 0$, $\mathrm{Re}E_n<0$) they should have an oscillatory exponential decrease. The boundary conditions can be satisfied by choosing appropriately the location of E_n on the Riemann sheet of $G(E_n)$. For open channels E_n should lie on the second sheet, just below the cut along the positive-energy axis, and for closed channels E_n should lie on the physical sheet, just below the negative-energy axis.

Equation (A1) is a (nonlinear) eigenvalue equation, determining $E^{(2)}$ and the zeroth Floquet component $\phi_0^{(2)}$; once this problem is solved, Eq. (A2) yields all other Floquet components. In practice, Eq. (A1) can be solved by taking into account that the terms V_1 and V_2 are perturbations, of first and second order in ω^{-1}, respectively. One can assume, preliminarily, that the eigenvalue $E^{(2)}$ is known and hence also the terms $V_1(E^{(2)})$ and $V_2(E^{(2)})$ are well defined. The problem being perturbative, the eigenvalue $E^{(2)}$ and eigenfunction $\phi_0^{(2)}$ are related to their unperturbed counterparts by the formulas of second-order standard perturbation theory, as given in [38], for example. Using these formulas, $E^{(2)}$ and $\phi_0^{(2)}$ are expressed in terms of matrix elements of $\overline{V_1}(E^{(2)})$ and $\overline{V_2}(E^{(2)})$, which obviously depend on $E^{(2)}$. Consistency to dominant order in ω^{-1} allows $E^{(2)}$ to be replaced in these matrix elements by its lower-order approximations, $E^{(1)}$ or W as the case may be. The result is [39]

$$E^{(2)}=W+\langle u|\overline{V_1}(E^{(1)})|u\rangle+\langle u|\overline{V_1}(W)G'(W)\overline{V_1}(W)|u\rangle+\langle u|\overline{V_2}(W)|u\rangle, \tag{A6}$$

$$\phi_0^{(2)}=[I+G'(E^{(1)})\overline{V_1}(E^{(1)})+G'(W)\overline{V_2}(W)+G'(W)\overline{V_1}(W)G'(W)\overline{V_1}(W)-\langle u|\overline{V_1}(W)|u\rangle G'^2(W)\overline{V_1}(W)]u. \tag{A7}$$

Here $G'(E)$ is the ''reduced'' form of $G(E)$; see [38] and [5], Eq. (64). $\overline{V_1}(W)$ and $\overline{V_2}(W)$ are calculated from Eqs. (A4) and (A5), with $G(E_n)$ replaced by $G(W_n)$. If $W+n\omega>0$, $G(W_n)$ represents a Green's function whose variable lies on the real positive axis of the energy [see Eq. (A3)]. To determine on which Riemann sheet of the Green's function W_n should lie, we recall that the original E_n lies on the second sheet just underneath the energy cut, which is close to $W_n+i\varepsilon$ on the physical sheet. Therefore, we should be dealing with $G^{(+)}(W_n)\equiv G(W_n+i\varepsilon)$ [25]. Further, we note that the first-order quasienergy $E^{(1)}$ entering Eqs. (A6) and (A7) is obtained by solving Eq. (A1) to first order (see [5], Sec. IV C) or, equivalently, by retaining only the first two terms in expression (A6) and replacing $E^{(1)}$ in $\overline{V_1}(E^{(1)})$ by $W+i\epsilon$.

Returning to Eq. (A2), consistency of the equation to second order in ω^{-1} allows $\phi_0^{(2)}$ to be replaced by its first-order expression resulting from Eq. (A7). Similarly, the operator $G_n(E^{(2)})$ acting on the bracket on the right-hand side of Eq. (A2) can be replaced by $G_n(E^{(1)})$, whereas the one inside the bracket, by $G_n(W)$. We find thus

$$\phi_n^{(2)}=G(E_n^{(1)})\left[V_n+V_nG'(W)\overline{V_1}(W)+\sum_m{}' V_{n-m}G^{(+)}(W_m)V_m\right]u \quad (n\neq 0). \tag{A8}$$

Formulas (A6)–(A8) are the result of the complete second-order iteration within the HFFT. As apparent, the successive iterations of the HFFT do not yield power series expansions in ω^{-1}, but rather expressions having their *dominant* terms of increasingly higher order in ω^{-1} (see also [5], Sec. IV B). If, on the other hand, one is working at really large ω such that Eq. (8) is quite well satisfied, one may eliminate from these formulas terms in ω^{-1} of higher order than the second. To this end one can use the fact, already mentioned, that at large ω, we have $G(E_n)\sim I(n\omega)^{-1}$. With the help of Eq. (5) one finds thus that the dominant behavior of the operator $V_1(E)$ is higher than the anticipated $O(\omega^{-1})$. Similarly, but with more bookkeeping, one can show that the dominant order of $\overline{V_2}(E)$ is higher than the anticipated $\underline{O(\omega^{-2})}$. Therefore, the terms containing twice the operator $V_1(W)$, as well as those containing $V_2(W)$, can be dropped in Eqs. (A7) and (A8). This gives the substantially simpler $O(\omega^{-2})$ formulas

$$E^{(2)}=W+\langle u|\overline{V_1}(E^{(1)})|u\rangle, \tag{A9}$$

$$\phi_0^{(2)}=[I+G'(E^{(1)})\overline{V_1}(E^{(1)})]u, \tag{A10}$$

$$\phi_n^{(2)}=G(E_n^{(1)})\left[V_n+\sum_m{}' \; V_{n-m}G^{(+)}(W_m)V_m\right]u \quad (n\neq 0). \tag{A11}$$

[1] See, for example, the volume *Atoms in Intense Laser Fields*, edited by M. Gavrila (Academic, New York, 1992).

[2] Applied in the strong-field context originally by Shih-I Chu and W. P. Reinhardt, Phys. Rev. Lett. **39**, 1195 (1977); see also Shih-I Chu, Adv. At. Mol. Phys. **21**, 197 (1985); Adv. Chem. Phys. **73**, 739 (1989); R. M. Potvliege and R. Shakeshaft, Phys. Rev. A **40**, 3061 (1989); **41**, 1609 (1990); and in *Atoms in Intense Laser Fields* (Ref. [1]), p. 373.

[3] Initiated by K. Kulander, Phys. Rev. A **35**, 445 (1987); **36**, 2726 (1987); **38**, 778 (1988); see also *Atoms in Intense Laser Fields*, Ref. [1], p. 247.

[4] (a) For free-free transitions see M. Gavrila and J. Z. Kaminski, Phys. Rev. Lett. **52**, 614 (1984); (b) for ionization see M. Gavrila, in *Fundamentals of Laser Interactions*, edited by F. Ehlotzky, Lecture Notes in Physics Vol. 229 (Springer, Berlin, 1985), p. 3.

[5] A systematic account of the HFFT for one-electron atoms was given by one of us (M.G.) in *Atoms in Intense Laser Fields* Ref. [1], p. 435.

[6] The relationship of the HFFT with the standard version of Floquet theory was studied recently by M. Marinescu and M. Gavrila, Phys. Rev. A **53**, 2513 (1996).

[7] (a) For atomic ground states, see M. Pont and M. Gavrila, Phys. Rev. Lett. **65**, 2362 (1990); (b) for Rydberg states, see R. J. Vos and M. Gavrila, Phys. Rev. Lett. **68**, 170 (1992); and also R. M. Potvliege and P. H. G. Smith, Phys. Rev. A **48**, R46 (1993). Both cases (a) and (b) are discussed by M. Gavrila, in *Atoms in Intense Laser Fields* (Ref. [1]), Sec. VI.

[8] For the Sturmian method, see M. Dörr, R. M. Potvliege, D. Proulx, and R. Shakeshaft, Phys. Rev. A **43**, 3729 (1991). For close coupling, see P. Marte and P. Zoller, *ibid.* **43**, 1512 (1991); L. Dimou and F. H. Faisal, *ibid.* **46**, 4442 (1992); **49**, 4564 (1994). For the *R* matrix method, see M. Dörr, P. G. Burke, C. J. Joachain, C. J. Noble, J. Purvis, and M. Terao-Dunseath, J. Phys. B **26**, L275 (1993).

[9] M. P. de Boer, J. H. Hoogenraad, R. B. Vrijen, R. C. Constantinescu, L. D. Noordam, and H. G. Muller, Phys. Rev. Lett. **71**, 3263 (1993); Phys. Rev. A **50**, 4085 (1994); N. J. van Druten, R. Constantinescu, J. M. Schins, H. Nieuwenhuizen, and H. G. Muller, *ibid.* **55**, 622 (1997).

[10] Dynamic stabilization was discovered for 1D models by Q. Su, J. H. Eberly, and J. Javanainen, Phys. Rev. Lett. **64**, 862 (1990); see also J. H. Eberly, R. Grobe, C. K. Law, and Q. Su, in *Atoms in Intense Laser Fields* (Ref. [1]), p. 301.

[11] 3D dynamic stabilization was shown by K. C. Kulander, K. J. Schafer, and J. L. Krause, Phys. Rev. Lett. **66**, 2601 (1991); see also *Atoms in Intense Laser Fields* (Ref. [1]), p. 247.

[12] V. V. Sviridov, Dokl. Akad. Nauk SSSR **274**, 1366 (1983) [Sov. Phys. Dokl. **29**, 139 (1984)]; see also P. Kuchment, *Floquet Theory for Partial Differential Equations* (Birkhäuser, Basel, 1993), Sec. 5.5.

[13] A rigorous analysis of the quasienergy spectrum for one-electron atoms was given by K. Yajima, Commun. Math. Phys. **87**, 331 (1982); S. Graffi and K. Yajima, *ibid.* **89**, 277 (1983), for the case of linear polarization; and A. Tip, J. Phys. A **16**, 3237 (1983), for the case of circular polarization. See also references therein.

[14] (a) V. C. Reed, P. L. Knight, and K. Burnett, Phys. Rev. Lett. **67**, 1415 (1991); (b) K. Burnett, V. C. Reed, and P. L. Knight, J. Phys. B **26**, 561 (1993).

[15] C. K. Law, Q. Su, and J. H. Eberly, Phys. Rev. A **44**, 7844 (1991).

[16] A. Sanpera, Q. Su, and L. Roso-Franco, Phys. Rev. A **47**, 2312 (1993).

[17] R. M. A. Vivirito and P. L. Knight, J. Phys. B **28**, 4357 (1995).

[18] Population analyses have also been made in WPD in terms of field-free states; e.g., see M. Dörr, O. Latinne, and C. J. Joachain, Phys. Rev. A **52**, 4289 (1995). Obviously, these populations have physical meaning only at the end of the pulse.

[19] Discovered repeatedly by W. Pauli and M. Fierz, Nuovo Cimento **15**, 167 (1938); see H. A. Kramers, *Collected Scientific Papers* (North-Holland, Amsterdam, 1956), p. 866; W. C. Henneberger, Phys. Rev. Lett. **21**, 838 (1968).

[20] The structure equation (6) was written down by W. C. Henneberger [19], but it was J. I. Gersten and M. H. Mittleman, J. Phys. B **9**, 2561 (1976), who recognized its high-frequency character.

[21] For continuum normalization in the energy scale, see E. Merzbacher, *Quantum Mechanics* (Wiley, New York, 1970), Chap. 6, Sec. 3.

[22] The condition $\alpha_0^2\omega\gg 1$, mentioned in [4(a)] and reproduced by others [e.g., in [14(b)]], has proven to be superfluous.

[23] Indeed, when properly normalized for integration (in the energy scale, for example), the continuum states have poles located at the discrete quasienergies.

[24] The proof was given by T. Berggren, Nucl. Phys. A **109**, 265 (1968), with the α-decay problem of nuclear physics in view. See also Berggren's contribution to the volume *Resonances*, edited by E. Brändas and N. Elander, Lecture Notes in Physics Vol. 325 (Springer, Berlin, 1988), p. 106, and other articles in the same volume for the background of the problem.

[25] The HFFT prescribes that matrix elements of $V_1(E^{(1)})$, or other operators containing Green's functions $G(E)$ at energies E on their second Riemann sheet, should be evaluated by analytic continuation from their counterparts defined on the real energy axis [see M. Gavila, in *Atoms in Intense Laser Fields* (Ref. [5]), Eqs. (89)–(91)]. The analytic continuation of the matrix elements can be achieved in practice by the ''regularization procedure'' described in [5], Sec. III A, i.e., the replacement of the potentials V_n by $V_n \exp(-\sigma x^2)$, and by taking the limit $\sigma \to 0$ at the end of the calculation. This procedure is equivalent to the Zeldovich-Berggren regularization procedure for Gamow states; see [24].

[26] Note that, in the laboratory frame and the velocity gauge, the dressed states are oscillating: $u_n^{(V)}(x) = u_n[x - \alpha(t)]$.

[27] J. Javanainen, J. H. Eberly, and Q. Su, Phys. Rev. A **38**, 3430 (1988).

[28] A. Dalgarno and J. T. Lewis, Proc. R. Soc. London, Ser. A **233**, 70 (1955).

[29] K. Smith, *The Calculation of Atomic Collision Processes* (Wiley, New York, 1971), Sec. 1.4.4.

[30] R. Kosloff, J. Phys. Chem. **92**, 2087 (1988).

[31] J. C. Wells, A. S. Umar, V. E. Oberacker, C. Bottcher, M. R. Strayer, J. S. Wu, J. Drake, and R. Flannery, Int. J. Mod. Phys. C **4**, 459 (1993).

[32] A. S. Umar and M. R. Strayer, Comput. Phys. Commun. **63**, 179 (1991).

[33] M. D. Feit, J. A. Fleck, Jr., and A. Steiger, J. Comput. Phys. **47**, 412 (1982).

[34] For the three cases considered (a) $\alpha_0 = 0.125$, (b) $\alpha_0 = 1.0$, and (c) $\alpha_0 = 5.0$, the values obtained for Γ are: at $\omega = 2$, (a) 2.88×10^{-4}, (b) 6.61×10^{-3}, and (c) 6.91×10^{-5}; at $\omega = 4$, (a) 6.7×10^{-5}, (b) 5.16×10^{-4}, and (c) 1.24×10^{-6}.

[35] At small intensities only one-photon ionization gives a sizable contribution to Γ: $\Gamma \cong \Gamma_1 \sim \alpha_0^2$.

[36] G. Yao and Shih-I Chu, Phys. Rev. A **45**, 6735 (1992).

[37] The matrix $T_{\alpha\nu}(0)$ is nonsingular because for $\omega^{-1} \to 0$ it reduces to the unit matrix and, by continuity, for small ω^{-1} (the case of interest), it maintains this property.

[38] For example, see A. Messiah, *Quantum Mechanics* (North-Holland, Amsterdam, 1962), Chap. XVI, Eqs. 5, 6, 10, 13, 14, 26, and 27. Note that our G' is denoted there by (Q_0/a).

[39] Equation (A6) coincides with Eq. (120) of [5], derived there otherwise.